UDC 621.372.8:621.391.63/4
*Indexing Terms:* Optical communications, Fibre optics, Single-mode transmission, Multimode transmission

# Optical fibre transmission lines

**Professor W. A. GAMBLING,** D.Sc., F.Eng., F.I.E.R.E.*

**A. H. HARTOG,** B.Sc.*

and

**C. M. RAGDALE,** M.A.*

**SUMMARY**

Optical fibre transmission lines have many advantages over coaxial cables. The most widely used fabrication techniques involve chemical vapour deposition resulting in losses of well below 1 dB/km. Analysis of propagation follows well-defined principles and the results obtained are broadly comparable with those at microwave frequencies, although the wavelength of operation, ~1 μm, is much shorter. By suitable design single-mode fibres can be made to give bandwidth × length products approaching 100 GHz · km. Multimode fibres are now well understood, pose fewer problems and can be excited with light-emitting diodes.

* *Department of Electronics, University of Southampton, Southampton, Hampshire SO9 5NH*

## 1 Introduction

The structure of optical fibre transmission lines takes the very simple form of a cylindrical glass core of refractive index $n_1$ surrounded by a cladding glass of refractive index $n_2$ where $n_2 < n_1$. Normally most of the propagating energy is contained in the core but there is always a radially-decaying evanescent field in the cladding, which may extend over several wavelengths in the case of single-mode fibres. Both core and cladding materials must therefore have very low absorption and scattering losses.

As with waveguides, when the transverse dimensions of the guiding structure, in this case the core, are comparable with a wavelength then only a single mode can be supported, whereas for larger core diameters multimode operation prevails. Section 2 indicates that the wavelength of operation is in the region of 1 μm, corresponding to a frequency of 300,000 GHz, so that *single-mode fibres* have a core diameter of 1 to 10 μm while *multimode fibres* have standardized core diameters of between 50 and 60 μm. For practical convenience the outer diameter is made 125 μm in both cases. In *step-index fibres* the refractive indices are constant in both core and cladding, whereas in (ideal) *graded-index fibres* the refractive index is a maximum $n_1$ at the core centre but falls monotonically to that of the cladding $n_2$ at the core boundary. With fibres designed for long-distance transmission $(n_1 - n_2) \ll n_1 \simeq 1{\cdot}5$ and the *relative refractive-index difference* $\Delta \simeq (n_1 - n_2)/n_1$ is about 1%.

At this point it is convenient to provide definitions of a few other basic quantities which are used in later Sections. Firstly, the maximum angle $\theta_m$ to the axis that light can enter a fibre at the input end from a medium of refractive index $n_0$ is defined in terms of the *numerical aperture NA* as

$$n_0 \sin \theta_m = NA = (n_1^2 - n_2^2)^{\frac{1}{2}} \simeq n_1(2\Delta)^{\frac{1}{2}} \qquad (1)$$

If the medium is air, for which $n_0 = 1$, and $\Delta = 0{\cdot}01$ then $\theta_m \simeq 12°$. The core radius $a$ is usually normalized to the free-space wavelength of operation $\lambda$ through

$$V = (2\pi a/\lambda)(n_1^2 - n_2^2)^{\frac{1}{2}} \simeq (2\pi a n_1/\lambda)(2\Delta)^{\frac{1}{2}} \qquad (2)$$

$V$ is called the *normalized frequency* although it could equally well be referred to as the normalized core diameter or normalized wavelength.

Why, one might ask, and under what circumstances, are optical fibres preferred to other forms of transmission line? Some of their merits and drawbacks are discussed in the following Sections, and other papers contained in this issue, but may be summarized as follows:

*Advantages*

1. Extremely low transmission loss (down to 0·2 dB/km) giving distances between repeaters in a trunk network, or in underwater cables, of 100 km and more, compared with 2 km for coaxial cables.



0033-7722/81/070313+13 $1.50/0

2. Extremely large bandwidths of up to 1 GHz·km for graded-index multimode fibres and 100 GHz·km for single-mode fibres, compared with ~20 MHz·km for coaxial cable.
3. Small size, low weight and high degree of flexibility.
4. Freedom from electromagnetic interference and earth-loop problems.
5. Fabricated from relatively abundant materials (silica, phosphorus, germanium, boron).
6. Zero cross-talk between closely-spaced lines.
7. Larger Young's modulus and resistance to crushing than copper.

*Disadvantages*

1. Glass is brittle and therefore breaks when the elastic limit is exceeded.
2. Long-term (20 years) mechanical stability under strain is unknown.
3. Demountable connectors and other similar components are expensive.

The properties of the principal types of optical fibre transmission line are summarized in Table 1.

The present paper attempts to do two things. Firstly, it outlines briefly the principal methods of fabrication, and the related attenuation characteristics, so that the properties of fibres can be more easily understood. Secondly, it describes the latest work, some of which has not been published elsewhere, on propagation in single-mode and multimode fibres. The details of the analyses are omitted but the principal steps and results are described in terms acceptable to the systems designer and practising engineer.

## 2 Fabrication of Optical Fibres

The glassy form of pure $SiO_2$ has an extremely low transmission loss in the optical and near-infra-red regions of the spectrum and can be drawn into long lengths with a high degree of precision. Silica, unfortunately, has the low refractive index of 1·45 and, when used as the core of a fibre, there are comparatively few compatible materials which have a sufficiently low refractive index to act as cladding. Possibilities are silica admixed with a small proportion of boron or fluorine and certain plastics such as silicone rubber. Conversely the index of silica can be raised by adding such oxides as $P_2O_5$, $GeO_2$ or $TiO_2$.

### 2.1 Chemical Vapour Deposition Techniques

Synthetic silica can be made by vapour deposition techniques involving oxidation or hydrolysis of volatile silicon compounds such as silicon tetrachloride or silane, which are liquids at room temperature. Methods of this kind are also used, but at very low deposition rates, in the semiconductor industry. Transition metal impurities, which cause high absorption, are largely excluded because the vapour pressures of their chlorides and hydrides are very much lower than those of silicon. Thus,

**Table 1**

Properties of optical fibres

| Type of fibre | | Core diameter (μm) | Materials | Transmission loss (dB/km) | | | | $B \times L$ product |
|---|---|---|---|---|---|---|---|---|
| | | | | 0·85 μm | 1·05 μm | 1·3 μm | 1·5 μm | GHz·km |
| Single-mode | | 1–10 | Core: silica based glass<br>Cladding: silica based glass | 2 | 1 | 0·38 | 0·2 | 50–100 |
| Multimode | Step-index | 50–200 | Core: silica based glass<br>Cladding: silica based glass | 2 | 1 | 0·5 | 0·2 | 0·005 to 0·02 |
| | | | Core: silica based glass<br>Cladding: plastic | 2·5 | 1·5 | high | | |
| | | | Core: multi-component glass<br>Cladding: multi-component glass | 3·4 | 6 | high | | |
| | Graded-index | 50–60 | Silica glass | 2 | 1 | 0·5 | 0·2 | 1 |
| | | | Multicomponent glass | 3·5 | 10 | high | | 0·4 |

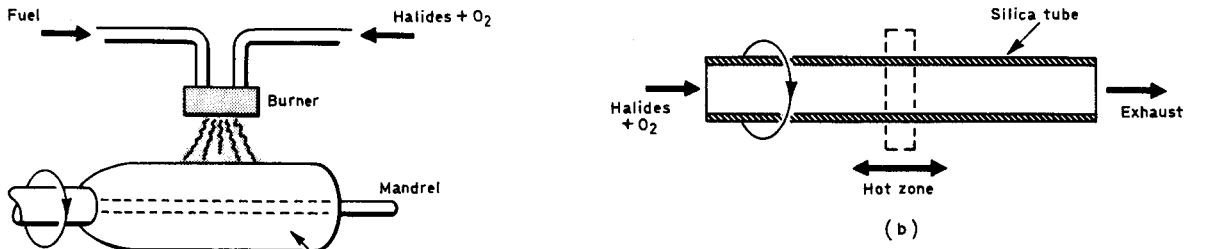


**Fig. 1.** Schematics of preform fabrication involving (a) soot deposition on the outside of a mandrel and (b) formation of glass layers on the inside of a tube.

when the appropriate silicon compound is vaporized by passing oxygen through it the impurities are left behind. If the mixture, now pure, is blown through an oxy-hydrogen flame then oxidation occurs and silica is generated as a fine soot which may be deposited on a cool mandrel. The oxidation reaction is the simple one: $SiCl_4 + O_2 \rightarrow SiO_2 + 2Cl_2$. When a sufficient thickness has been deposited the mandrel is removed and the porous mass of silica soot is then sintered and collapsed into solid glass.

The process can be adapted to the fabrication of fibres by starting with a mixture of two vapours such as $SiCl_4$ and $GeCl_4$, together with oxygen, as in Fig. 1(a). The mandrel is rotated and traversed in the longitudinal direction under the flame from the burner, so that the corresponding oxides deposit as a fine, mixed, porous soot on the mandrel.[1] When a sufficient thickness has been achieved the gas composition is changed so that a soot of the mixed cladding oxides forms a second layer. The mandrel is then removed and the soot preform is carefully sintered into a solid composite preform which is drawn into fibre. This technique is often referred to as Outside Vapour Phase Oxidation (OVPO) and is one of the general class of Chemical Vapour Deposition (CVD) methods.

The method most widely used involves deposition on the inside of a tube in such a way that soot formation and sintering are simultaneous. It was developed independently at Southampton University[2] and Bell Telephone Laboratories[3] and is known as the modified, or homogeneous, CVD process (sometimes as the Inside Vapour Phase Oxidation or IVPO process). The tube is usually of high-quality silica, having uniform thickness and good circularity. This tube can form the cladding material but more usually acts simply as a supporting structure. In that case a low-loss silica cladding can be produced by picking up the vapour of silicon tetrachloride by bubbling oxygen through the liquid and passing the mixture along the tube, as in Fig. 1(b). By heating the tube with an outside heat source, usually a flame, the oxidation reaction again produces a fine soot of silica but it now, in the homogeneous or modified CVD method, deposits and sinters into a clear glass layer on the wall of the tube. The thickness may be up to 10 μm. In order to ensure uniformity the heating torch is traversed in the longitudinal direction and the tube is rotated. When a sufficient total thickness has been formed by successive traverses of the torch the vapours of the chlorides of phosphorus ($POCl_3$) or germanium ($GeCl_4$) are added to the flow and layers of phosphosilicate or germanosilicate glass are deposited to form the core glass. The deposition temperature is in the region of 1500 to 1600°C. In practice boric oxide (from $BCl_3$) or fluorine is added to the silica cladding to produce a lower refractive index and a lower deposition temperature which reduces tube distortion.

The second stage of the process is to raise the temperature of the torch so that the composite tube softens and surface tension forces cause it to collapse into a solid rod.[4] Usually two or three passes of the flame are sufficient. Finally the preform is mounted vertically and is drawn into a fibre in a fibre-drawing machine, where a short section at one end of the rod is heated to softening temperature. The lower end is pulled downwards at a constant velocity of the order 1 m/s and the resulting fibre diameter is determined by the ratio of the fibre drawing speed to the rate at which the preform is fed into the furnace. A great advantage of the CVD methods, especially the homogeneous (inside) process is that the composition of successive layers can be changed thus producing a graded refractive-index distribution.

The methods described so far are essentially batch processes in that a preform is made and then drawn into a finite length, up to 10 km, of fibre. A more recent development is that, instead of depositing the glass soot on the outside cylindrical surface of the mandrel as in the OVPO method, it is deposited on the end of the rotating boule. By slowly withdrawing the boule in the longitudinal direction at the same rate as the deposition builds up a continuous process results. This is the basis of the Vapour Phase Axial Deposition (VAD) method.[5]

### 2.2 Multicomponent Glass Fibres

An alternative method of making fibres involves multicomponent glasses, such as sodium borosilicate, which can be worked at the much lower temperatures of 900–1300°C. A double-crucible arrangement[1], as in Fig. 2, is normally used. Core glass is melted in the inner crucible and cladding glass in the outer, and they flow through the nozzles to form a fibre. This method may be

suitable for mass production but care has to be taken to prevent impurities entering from the crucibles and it is difficult to obtain starting materials of the required quality. Great care must therefore be taken during preparation.

As shown in Table 1, multimode fibres with both a step-index and a graded-index, including parabolic, distribution in the core have been produced from multicomponent glasses. The loss has recently been reduced to less than 3·5 dB/km at a wavelength of 0·85 μm but it rises rapidly beyond 1 μm. A graded distribution can be obtained with the double-crucible method by allowing diffusion of ions, and therefore an ion exchange, after the core glass has emerged from the inner nozzle.

The Rayleigh scattering loss may be smaller in certain compound glasses, but unfortunately multicomponent scattering is increased.

### 2.3 Other Fabrication Methods

There are a number of other fabrication processes which cannot all be mentioned here. Generally the losses in the resulting fibres are higher but this may not be important in short-distance applications.

A simple process is to insert a rod of core glass into a tube of cladding glass and to draw the combination into fibre. In another variation a silica rod is drawn into fibre and coated with a suitable plastic, of lower refractive index, which forms the cladding.[4]

### 2.4 Transmission Loss of Optical Fibres

The factors contributing to loss in an optical fibre transmission line include absorption, scattering due to inhomogeneities in the core refractive index (Rayleigh scattering), scattering due to irregularities at the boundary between core and cladding, bending loss, loss at joints and connectors and the coupling losses at the input and output.

Remarkable progress has been made in reducing the transmission loss, which has fallen by about three orders of magnitude in the past ten years and is now much lower than that of coaxial cables having a similar transmission bandwidth. The absorption loss at some wavelengths is almost negligible and below about 0·8 μm scattering is the dominant factor.

The main cause of the absorption loss is the presence of transition metals such as Fe, Cu (especially in multicomponent glasses), water in the form of $OH^-$ ions and the intrinsic absorption of the pure glass itself. In order to reduce the absorption to an acceptable level, it is necessary to prevent a metal concentration of more than 1 in $10^9$, and an OH radical concentration of more than 1 in $10^7$, from occurring.

Another purely material effect in addition to absorption is the scattering due to inhomogeneities of the refractive index. These fluctuations are on a scale

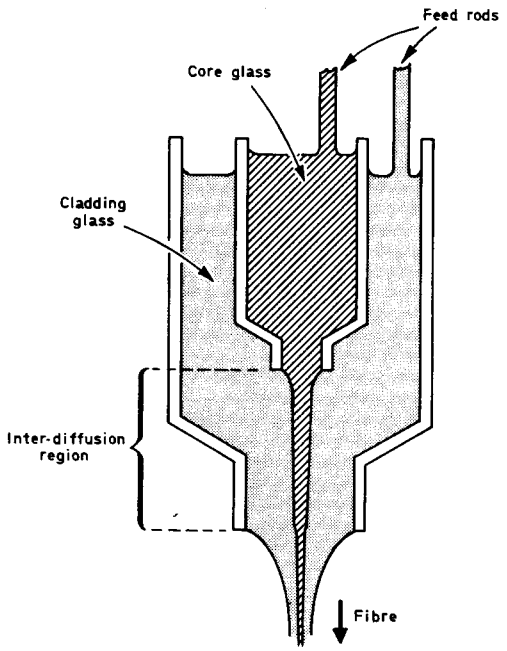


**Fig. 2.** Fibre drawing with double crucible showing diffusion zone for producing a graded refractive index.

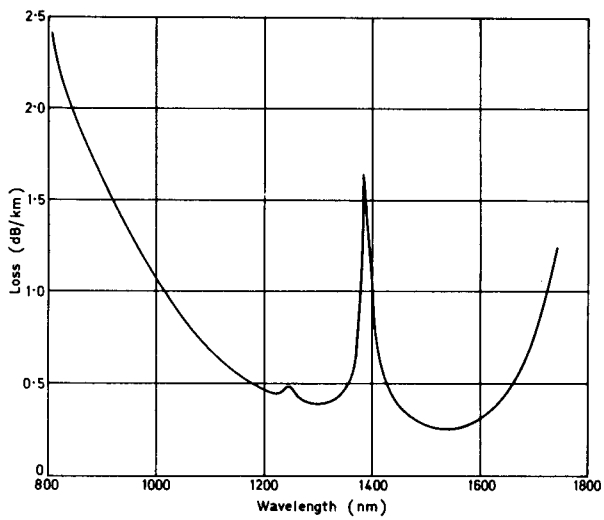


**Fig. 3.** Transmission loss of a single-mode fibre with a germanosilicate core of 10·5 μm diameter and phosphofluorosilicate cladding. Peaks due to $OH^-$ are present at 1·24 and 1·39 μm.

which is smaller than the wavelength and the resulting Rayleigh scattering is inversely proportional to the fourth power of the wavelength ($\lambda^{-4}$), so that it becomes rapidly smaller at longer wavelengths.

The transmission of a single-mode fibre† with a germanosilicate core and phosphofluorosilicate cladding is shown in Fig. 3 and exhibits the characteristic features of fibres made by the modified CVD process. In this particular case the core diameter is 10·5 μm, the relative

† K. J. Beales (Private Communication).

refractive-index difference is $\Delta = 0{\cdot}17\%$ and the cut-off wavelength of the second set of modes ($TM_{01}$, $TE_{01}$ and $HE_{21}$) is 1·2 μm. At short wavelengths the attenuation is inversely proportional to the fourth power of the wavelength and is therefore typical of Rayleigh scattering.

The rise in attenuation beyond 1·7 μm is attributed to the intrinsic infra-red absorption of the glass. The effect of $OH^-$ impurities can be clearly seen but are at a much lower level than is normally observed. The fundamental vibration is at $\lambda = 2{\cdot}8$ μm in silica and there are overtones at 1·39 μm and 1·24 μm.

The transmission loss at 1·3 μm of 0·38 dB/km is the lowest yet reported at that wavelength and is 0·28 dB/km at 1·55 μm. The fibre illustrated in Fig. 3 was designed for operation at 1·3 μm but it has been shown that in other fibres[6] the loss at 1·55 μm can be as low as 0·2 dB/km. Large transmission distances are therefore possible (see Table 1), and British Telecom are already designing single-mode fibre systems operating at 1·3 μm over repeater spacings of 30 km at 140 Mbit/s.

A mode conversion loss, and a loss due to radiation, occur if the fibre has small irregularities at the boundary between the core and cladding. However, this interface scattering, which is referred to as 'microbending', can be reduced by increasing both the core radius and the index gradient in the core in order to minimize the light intensity at the core/cladding boundary.

Bends can also cause mode conversion to occur in addition to the energy loss due to radiation.

## 3 Propagation in Single-mode Fibres

The analysis of optical fibres follows the same procedure as that for any other transmission line which guides electromagentic waves. Thus solutions of Maxwell's equations and the corresponding wave equation are sought in terms of the appropriate boundary equations, using well-established techniques. For each of the propagating modes it is possible to deduce the spatial distribution of the electric and magnetic fields, the propagation constant, phase and group velocities, and so on, in the normal way. Optical fibres differ in degree only and not in principle from, say, hollow metal waveguides, in that they are designed for operation at frequencies higher by a factor of $10^4$ and the guiding structure is fabricated entirely from dielectric materials since metals are very lossy at optical frequencies.

### 3.1 Basic Concepts

A dielectric waveguide supports a finite number of guided modes and an infinite number of radiation modes which together form a complete orthogonal set. Only guided modes are considered here.

To simplify the analysis of fibre waveguides the cladding may be assumed to be of infinite extent. In practice this simply means that the cladding diameter must be large enough for the field to decay to a negligible level at its outer edge. In single-mode fibres a significant proportion of the power is carried in the cladding which must have a diameter roughly seven times that of the core, say 30 μm.

An exact description of the modal fields is complicated, but the analysis can be simplified by making use of the fact that, in practice, $(n_1 - n_2) \ll n_1$, the well-known 'weakly-guiding approximation'. The approximate mode solutions derived in this way are very nearly linearly-polarized[7,8] and are denoted by $LP_{\nu\mu}$ where $\nu$ and $\mu$ denote the zeros of the field in the azimuthal and radial directions respectively. These linearly-polarized modes correspond to a superposition of the two modes $HE_{\nu+1,\mu}$ and $EH_{\nu-1,\mu}$ of the exact solution of Maxwell's equations. The exact modes are nearly degenerate and as $n_2 \to n_1$ their propagation constants become identical.

Maxwell's equations with the weakly-guiding approximation give the scalar wave equation as:

$$\frac{d^2\psi}{dr^2} + \frac{1}{r}\frac{d\psi}{dr} + \frac{1}{r^2}\frac{d^2\psi}{d\phi^2} + [n^2(r)k^2 - \beta^2]\psi = 0 \qquad (3)$$

where $\psi$ is the field (E or H), $k = 2\pi/\lambda$ is the free-space wave number, $n(r)$ is the radial variation of the refractive index and $r$, $\phi$ are the cylindrical co-ordinates. The propagation constant $\beta$ of a guided mode obviously lies between the limits $n_2 k < \beta < n_1 k$. The fibre is circular in cross-section and the solutions of the wave equation are separable, having the form:

$$\psi = E(r)\cos\nu\phi \exp[j(\omega t - \beta z)] \qquad (4)$$

For simplicity the factor $\exp[j(\omega t - \beta z)]$ will be omitted from later equations.

In single-mode fibres only the fundamental $LP_{01}$ mode propagates and it has no azimuthal dependence, i.e. $\nu = 0$. It corresponds to the $HE_{11}$ mode derived from the exact analysis. For this fundamental mode equation (3) reduces to

$$\frac{d^2E}{dr^2} + \frac{1}{r}\frac{dE}{dr} + [n^2(r)k - \beta^2]E = 0 \qquad (5)$$

In a step-index fibre, i.e. one with a constant refractive index $n_1$ in the core, equation (5) is Bessel's differential equation and the solutions are cylinder functions. The field must be finite at $r = 0$ and therefore in the core region the solution is a Bessel function $J_\nu$. Similarly the field must vanish as $r \to \infty$ so that the solution in the cladding is a modified Bessel function $K_\nu$. For the fundamental $LP_{01}$ mode polarized in either the $x$ or $y$ direction the field is therefore[7]

$$E(r) = AJ_0(UR) \quad R < 1 \quad \text{(core)}$$
$$= AJ_0(U)\frac{K_0(WR)}{K_0(W)} \quad R > 1 \quad \text{(cladding)} \qquad (6)$$

where $R = r/a$ is the normalized radial coordinate and $A$

is the amplitude coefficient. $U$ and $W$ are the eigenvalues in the core, and cladding, respectively and are defined by

$$U^2 = a^2(n_1^2k^2 - \beta^2) \tag{7}$$
$$W^2 = a^2(\beta^2 - n_2^2k^2)$$

therefore

$$V^2 = a^2k^2(n_1^2 - n_2^2) = U^2 + W^2$$

Related to these parameters is the normalized propagation constant $b$, defined as[8]

$$b = [(\beta/k)^2 - n_2^2]/2n_1^2\Delta = 1 - \frac{U^2}{V^2} \tag{8}$$

where

$$\Delta = \frac{n_1^2 - n_2^2}{2n_1^2} \simeq \frac{n_1 - n_2}{n_1} \ll 1$$

Since, for a guided mode, the limits of $\beta$ are $n_2k$ and $n_1k$ then $b$ must lie between 0 and 1.

The field expressions in equation (6) are normalized so as to have the same value at $r = a$. In addition the tangential electric field components must be continuous at this point, leading to the following eigenvalue equation for the $LP_{01}$ mode:

$$\frac{UJ_1(U)}{J_0(U)} = \frac{WK_1(W)}{K_0(W)} \tag{9}$$

It should be noted that it is only because of the weak-guidance approximation that the boundary conditions of the magnetic field components are also satisfied by this condition.

By solving equations (7) and (9) the eigenvalue $U$, and hence $\beta$, can be calculated as a function of the normalized frequency $V$. Therefore the dependence of the propagation characteristics of the mode on the wavelength and fibre parameters can be determined.

At the lower limit of $\beta = n_2k$ the mode phase velocity equals the velocity of light in the cladding and is no longer guided, the mode is cut off and the eigenvalue $W = 0$ (equation (7)). As $\beta$ increases, less power is carried in the cladding and at $\beta = n_1k$ all the power is confined to the core.

The limit of single-mode operation is determined by the wavelength at which the propagation constant of the second, $LP_{11}$, mode equals $n_2k$. For a step-index fibre this cut-off condition is given by

$$J_0(V_c) = 0$$

where $V_c$ denotes the cut-off value of $V$ which, for the $LP_{11}$ mode, is equal to 2·405. The fundamental mode has no cut-off, hence single-mode operation is possible for $0 \leqslant V \leqslant 2{\cdot}4$.†

† The reader is invited to deduce, from simple physical principles, the consequences of operating in practice at too low a value of $V$.

### 3.2 Dispersion in Single-mode Fibres

The bandwidth of optical fibres is limited by broadening of the propagating light pulse which has a finite spectral width due to (i) the spectral width of the source, and (ii) the modulation sidebands of the signal. If, therefore, the fibre waveguide is dispersive the different frequency components will travel at different velocities resulting in pulse distortion.

The transit time for a light pulse propagating along a fibre of length $L$ is

$$\tau = \frac{L}{c}\frac{d\beta}{dk} \tag{10}$$

where $c$ is the velocity of light.

If $\beta$ varies non-linearly with wavelength the fibre will be dispersive. From equation (8) we have

$$\beta^2 = k^2n_1^2[1 - 2\Delta(1 - b)] \tag{11}$$

Thus $\beta$ is a function of the refractive indices of the core and cladding materials and of $b$. Equation (8) shows that $b$ is a function of $V$ so that pulse dispersion arises from the variation of $b$ with the ratio $a/\lambda$. In addition, the refractive index of the fibre material varies non-linearly with wavelength and this also gives rise to pulse dispersion.

The pulse spreading caused by dispersion is given by the derivative of the group delay with respect to wavelength[9]

$$\text{pulse spread} = \left|\delta\lambda\frac{d\tau}{d\lambda}\right| L = \frac{L}{c}\frac{2\pi}{\lambda^2}\frac{d^2\beta}{dk^2}\delta\lambda \tag{12}$$

where $\delta\lambda$ is the spectral width of the source. Substituting equation (11) into equation (12), and differentiating with respect to $k$, gives the dependence of the pulse spreading on the material properties and the mode parameter $b$. The dependence on the refractive index is given in terms of the material dispersion[9] parameter $-(\lambda/c)(d^2n/d\lambda^2)$ where $n = n_1$ or $n_2$ and the dependence on $b$ is given by the mode dispersion parameter defined as $V(d^2(bV)/dV^2)$. In addition a third term, which is proportional to $d\Delta/d\lambda$, arises from the differentiation in equation (12).

The preceding three effects are inter-related in a complicated manner, but Reference 10 shows that the expression for pulse spreading can be separated into three composite dispersion components in such a way that one of the effects dominates each term. For example, a composite material dispersion term can be defined which has a dependence on both $b$ and $d^2n/d\lambda^2$, however it becomes zero when $d^2n/d\lambda^2$ is zero.

In multimode fibres the majority of the modes are far from cut off and most of the power is carried in the core. In this case the composite dispersion components simplify to terms which depend on either material or mode dispersion, and the two effects can be separated. In addition, in step-index multimode fibres the effect of $d\Delta/d\lambda$ can be neglected.

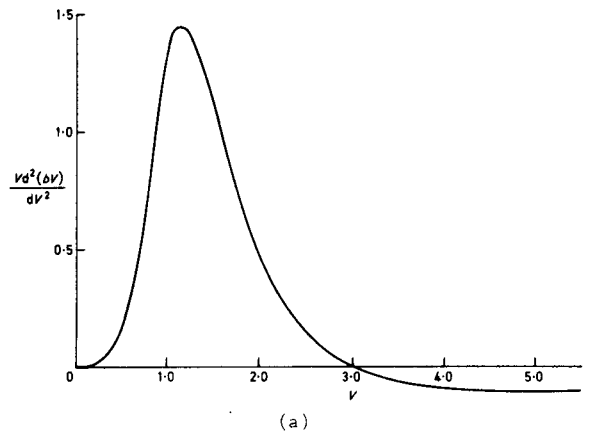


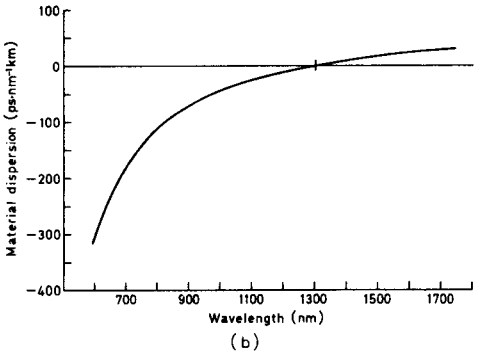


**Fig. 4.**(a) The mode dispersion parameter, $V(d^2(bV))/dV^2$ as a function of normalized frequency $V$ for the fundamental $LP_{01}$ mode.
(b) The material dispersion parameter, $-(\lambda/c)(d^2n/d\lambda^2)$ as a function of wavelength for a germanosilicate glass fibre with $NA = 0{\cdot}2$.

Material and mode dispersion also have a dominant effect in single-mode fibres but the effect of $d\Delta/d\lambda$ can no longer be neglected[10] as has been assumed by some authors.

In the absence of material dispersion the pulse spreading is controlled by the mode parameter $Vd^2(bV)/dV^2$ which is shown in Fig. 4(a) as a function of $V$ for the $LP_{01}$ mode. In the single-mode regime, i.e. $V < 2{\cdot}4$, the mode dispersion is always positive and reaches a maximum at $V = 1{\cdot}15$. It is seen that a change in any of the waveguide parameters, e.g. core radius or wavelength, changes $V$ and hence the mode dispersion.

The material dispersion parameter, $(\lambda/c)(d^2n/d\lambda^2)$ is plotted as a function of wavelength in Fig. 4(b) for a germanophosphosilicate glass fibre with $NA = 0{\cdot}2$. At most wavelengths the material dispersion exceeds mode dispersion, but at 1·29 μm the material dispersion is zero[9] (i.e. $d\tau/d\lambda = 0$). Thus at wavelengths near this value the bandwidth is limited by mode dispersion.

The total dispersion of a single-mode fibre arises from the combined effects of material dispersion, mode dispersion and $d\Delta/d\lambda$ terms. As shown in Fig. 4(b) the material dispersion function changes sign at a wavelength of approximately 1·29 μm whereas mode dispersion always has the same sign in the single-mode regime. Therefore the effects of material dispersion, $d\Delta/d\lambda$ and mode dispersion can be balanced to give zero first-order dispersion at a given wavelength.[10] Hence extremely large bandwidths can, in theory and practice, be achieved in single-mode fibres.

Since the dispersive properties of the fibre depend on both the fibre core dimensions and the fibre materials the total dispersion can be altered by changing either of these parameters. The wavelength $\lambda_0$ at which the first-order dispersion is zero can therefore be tuned by appropriate choice of the core diameter or of $NA$. The total dispersion is plotted in Fig. 5 as a function of wavelength for different core diameters and a fixed $NA$ of 0·23.

The range of wavelengths over which $\lambda_0$ can be tuned is limited. The maximum value depends on the usable value of $NA$, while the minimum value is approximately the wavelength at which material dispersion is zero ($\sim 1{\cdot}3$ μm).

If a fibre is designed to operate with zero first-order dispersion the limitations imposed on the bandwidth by secondary effects must be considered. For example, birefringence arising from ellipticity or stress in the core causes the two orthogonally-polarized modes of the 'single-mode fibres' to become distinguishable, i.e. they are no longer degenerate as in the scalar approximation.[11,12] The modes have different propagation constants which results in pulse dispersion. The dispersion caused by a difference between the major and minor axes of about 5% is less than 2 ps/km and can therefore be neglected.[11] On the other hand the pulse dispersion arising from stress birefringence may be as high as 40 ps/km if the expansion coefficients between the fibre core and cladding materials are not matched.[13]

Figure 6 shows the bandwidth of a single-mode fibre designed for $\lambda_0 = 1{\cdot}3$ μm. In the absence of second-order

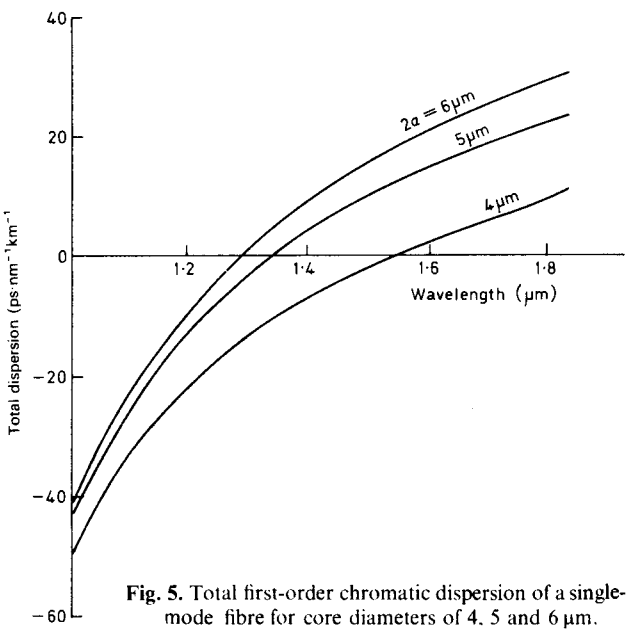


**Fig. 5.** Total first-order chromatic dispersion of a single-mode fibre for core diameters of 4, 5 and 6 μm.

effects the bandwidth is limited only by the spectral width of the source. Thus the solid line shows the available bandwidth with a source of linewidth 1 nm (e.g. an oxide stripe laser). On the other hand if stress birefringence introduces a pulse dispersion of 10 ps/km the bandwidth in the vicinity of $\lambda_0$ is considerably reduced (dotted curve). In the absence of polarization dispersion the bandwidth near $\lambda_0$ would be determined by higher-order effects.

Further work on this topic is required but preliminary measurements with a narrow-linewidth laser source over a 20 km length have revealed† a pulse dispersion of less than 4 ps/km.

### 3.3 Spot Size

The spot size of the fundamental mode is one of the most important parameters in single-mode fibre design since it largely determines the launching efficiency, jointing loss and bending loss. Usually the spot size $w_0$ is defined as the width to 1/e intensity of the $LP_{01}$ mode or, alternatively, in terms of the spot size of an incident Gaussian beam which gives maximum launching efficiency.[14] The latter definition arises from the fact that the $LP_{01}$ mode has almost a Gaussian distribution.

The spot size is a function of both $V$ and $NA$, although the dependence on $V$ is only slight[14] ($w_0$ changes by only 2% over the range $V = 1{\cdot}8$ to $2{\cdot}4$). The numerical aperture, on the other hand, has a strong effect since a large $NA$ increases the guidance effect and more of the power in the $LP_{01}$ mode is confined to the core, so that the spot size decreases.

### 3.4 Launching Efficiency

The ratio of power accepted by the fibre to the power in an incident beam is defined as the launching efficiency and can be calculated by integrating the product of the incident and propagating modes over the fibre cross-section.[15]

Thus launching efficiency

$$= \frac{1}{n_1}\left|\int^A E_{\text{inc}} \cdot E \, dA\right|^2 / \int^A E_{\text{inc}}^2 \, dA \int^A E^2 \, dA \qquad (13)$$

where $E_{\text{inc}}$ is the electric field distribution of the incident mode.

Maximum power is launched into the fibre when the spot size of the $LP_{01}$ mode is matched to the waist of the incident Gaussian beam. In practice, however, the launching efficiency of the $LP_{01}$ mode decreases if the input beam is offset or tilted.

### 3.5 Joint Loss

The efficiency with which power can be coupled between two fibres is determined by the extent to which the mode patterns of the incoming and outgoing fibres can be matched. Therefore angular or lateral misalignment can considerably increase the loss at a joint. While longitudinal separation between the ends of the fibres can also occur its effect on loss in practical joints is small enough to be neglected.

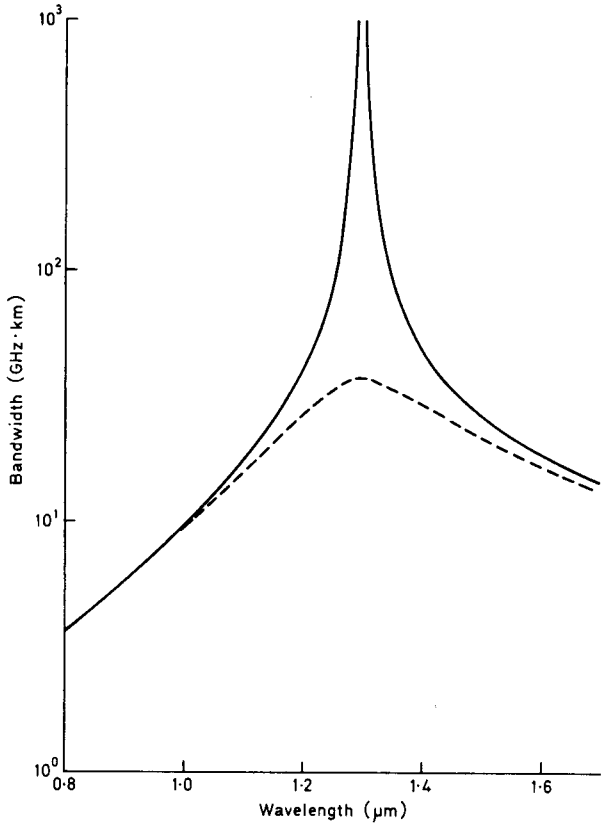


**Fig. 6.** Bandwidth of a single-mode fibre designed for $\lambda_0 = 1{\cdot}3$ μm, assuming a source linewidth of 1 nm and that second-order effects are small. The dotted curve shows the effect of a polarization dispersion of 10 ps/km.

If it is assumed that the spot sizes of the modes of the two fibres are the same then the joint loss can be derived simply in terms of spot size. In the absence of angular misalignment the loss caused by lateral offset[16] is

$$T_l = 2{\cdot}17\,(D/w_0)^2 \text{ dB} \qquad (14)$$

where $D$ is the offset. The offset loss is thus inversely proportional to the square of the spot size, $w_0$. On the other hand the loss caused by an angular misalignment $\alpha$ is

$$T_a = 2{\cdot}17\,(\alpha w_0 nV/aNA)^2 \text{ dB} \qquad (15)$$

and hence angular misalignment loss is directly proportional to the square of the spot size. Thus for a given loss there is a trade-off between the spot size, and hence $NA$, required for low offset loss and that required for low angular misalignment loss.

When angular and lateral misalignments occur together the combined effect is complicated,[16] but if the total loss is small it can be approximated by the sum of equations (14) and (15).

† K. J. Beales (Private communication).

### 3.6 Bending Loss

Radiation at bends in single-mode fibres can significantly increase the transmission loss.[17-20] The bending loss can arise either from curvature of the fibre axis or microbending, i.e. small inhomogeneities in the fibre such as diameter variations, which can arise during coating and cabling.

There are two different mechanisms giving rise to bend loss in single-mode fibres, namely transition loss and pure-bend loss.[19,20] The transition loss is oscillatory and arises because power is lost by coupling between the fundamental mode and the radiation modes. In other words the power distribution in the $HE_{11}$ mode of the straight fibre is different from that of the corresponding mode in the curved fibre and power is lost at the interface between the two due to this mismatch.

The second mechanism, pure-bend loss, represents a loss of energy from the pure mode of the curved fibre and can be explained as follows. At a bend the phase fronts are no longer parallel and at a sufficiently large distance from the centre of curvature the increased distance between the phase fronts corresponds to a phase velocity greater than $c/n_2$. This part of the wave is no longer guided and radiates away from the fibre. As the curvature is increased the radius at which the phase velocity equals the velocity of light decreases, hence more energy is lost. The amount of power radiated depends on the spot size. If the spot size is reduced the power is more tightly guided in the core and the pure-bend loss decreases.

Both the transition loss and pure bend loss are strongly dependent on the $NA$ (and hence the spot size). It is therefore possible to reduce bending loss to a negligible level by increasing the numerical aperture of the fibre.

### 3.7 Arbitrary Profiles

In the discussions above only a stepped refractive-index profile has been considered. In practice, however, the real profiles of single-mode fibres have a dip in the centre and some grading of the core/cladding boundary caused by diffusion of dopants during the fabrication process. In addition the refractive index in the cladding is not usually constant. The field distribution and propagation characteristics of the $LP_{01}$ mode are thus different quantitatively, although not qualitatively, from those in the step-index fibre. Hence all of the properties discussed above will be different for fibres with different profiles.

There are two ways of dealing with this problem. The first is to use the measured refractive-index profile to produce a numerical solution[21] of the scalar wave equation (equation (3)). The second method involves matching the mode field of the real fibre to that of a fibre with equivalent step-index distribution.[22-24] This simplifies the problem since the analytical expressions for a step-index fibre can be used; however, it is not very accurate for fibre profiles which depart too far from a stepped distribution.

## 4 Propagation in Multimode Fibres

### 4.1 Basic Concepts

Although single-mode fibres have intrinsically higher bandwidths than those offered by multimode fibres, much of the research and development in optical communications has, until recently, concentrated on the latter type of waveguide. Multimode fibres have larger core diameters and numerical apertures than single-mode fibres and, as a result, can be coupled more easily to optical sources. In particular, light-emitting diodes, which are cheaper and more reliable than lasers, can be used to drive multimode fibre links. Moreover jointing and splicing losses are much lower than with single-mode fibres since the dimensions are larger and hence the alignment tolerances are much less stringent. Finally, multimode fibres are less susceptible to microbending losses.

Typical multimode fibres have a core diameter of 50 μm, a numerical aperture of 0·2 (i.e. a relative index difference $\Delta$ of slightly less than 1%) and an outer diameter of 125 μm. At a wavelength of 0·85 μm (the emission wavelength of GaAs devices) the corresponding normalized frequency is $V = 37$ and the number of guided modes (approximately $V^2/4$ for graded-core fibres) is $\sim 340$.

In general, therefore, power is launched into a large number of modes having different spatial field distributions, propagation constants, chromatic dispersion and so on. In an ideal fibre, having properties (e.g. core size, index difference, refractive-index profile) which are independent of distance, then the power launched into a given mode remains in that mode and travels independently of the power launched into other modes. In addition most of the modes are operated far from cut-off and their properties are, therefore, relatively independent of wavelength. This behaviour contrasts with single-mode operation where the mode parameters, such as normalized propagation constant or power confinement factor, vary rapidly with wavelength.

Since the majority of modes operate far from cut-off, and are thus well confined, most of the power carried by multimode fibres travels in the core region. The properties of the cladding therefore only significantly affect those modes which are near cut-off and whose electromagnetic fields extend appreciably beyond the core.

### 4.2 Intermodal Dispersion

The existence of several hundred modes, each having its own propagation constant, causes a form of pulse distortion which does not exist in single-mode fibres, namely intermodal dispersion. The energy of an impulse launched into a multimode fibre is therefore spread over

a time interval corresponding to the range of propagation delays of the modes. The number of signal pulses which may be transmitted in a given period, and hence the information-carrying capacity of the fibre, is therefore reduced. Since, in the absence of mode filtering or mode conversion, the pulse spreading increases linearly with fibre length, the bandwidth is inversely proportional to distance. The product of bandwidth $B$ and distance $L$ is therefore a figure of merit for the information capacity of an optical fibre. For example, Table 1 shows that the $B \times L$ product for a step-index fibre is typically 20 MHz·km. As indicated in the Introduction, a careful choice of the radial variation of the refractive index enables the transit-times of the modes to be almost equalized so that $B \times L$ products of 10—20 GHz·km have been predicted although not yet achieved in practice. The power-law, or $\alpha$, class of refractive-index profiles, given by

$$n^2(r) = n_1^2\left[1 - 2\Delta\left(\frac{r}{a}\right)^\alpha\right] \qquad r < a$$
$$n^2(r) = n_1^2[1 - 2\Delta] = n_2^2 \qquad r > a \tag{16}$$

has been used extensively to model the grading function of multimode fibres. The profile is optimized by a suitable choice of $\alpha$. It may be shown [25,26] that, neglecting the dispersive properties of the glasses forming the waveguide, the value of $\alpha$ which minimizes the r.m.s. pulse broadening is given by

$$\alpha_{opt} = 2 - \frac{12\Delta}{5} \tag{17}$$

and the r.m.s. output pulse width produced by a unit impulse at the input is then:[26]

$$\sigma_{opt} = \frac{L}{c}\frac{n_1}{20\sqrt{3}}\Delta^2 \tag{18}$$

The intermodal dispersion is, however, an extremely sensitive function of the index-profile. Minute departures of refractive index from the power law, or an incorrect design of the profile, lead to a much lower bandwidth than is theoretically achievable. For example, an error in $\alpha$ of $\sim 1\%$ degrades the bandwidth by a factor of two. The central dip caused by dopant evaporation in the high-temperature collapse stage of the CVD process, and the step-like structure caused by the deposition of individual glass layers, have been shown to contribute significantly to the pulse broadening. Nevertheless extremely high $B \times L$ products have been achieved using several variants of the CVD process and the best results reported in the literature are summarized in Table 2.

It may be seen that the best value is within a factor of 2 of the maximum predicted for $\alpha$ profiles, but whether fibres of this quality can be prepared under routine production conditions remains to be seen.

### 4.3 Effect of the Wavelength Dependence of Refractive Index

The variation of refractive index with wavelength also causes the transmitted pulses to broaden, as we have seen in the case of single-mode fibres. With multimode fibres an additional, more subtle, effect exists since the index dispersion $dn/d\lambda$ also alters the relative transit-times of the modes and hence, the intermodal dispersion.[26] This is normally referred to as 'profile dispersion' and is a result of the difference which exists between the group index $N = n - \lambda(dn/d\lambda)$ (which determines the pulse transit time) and the refractive index $n$.

Since $dn/d\lambda$ is, in general, a function of glass composition it varies across the core of a graded-index fibre. Hence each mode is affected differently by dispersion since the spatial distribution of power is not the same for all modes. For example, low-order modes travel, on average, in a medium of higher dopant concentration than do higher-order modes. Thus a correction to the optimum profile parameter is required to account for the difference between the functions $N_1(r)$ and $n_1(r)$. Olshansky and Keck[26] extended the analysis of power-law profiles to include the effect of glass dispersion and showed that in the presence of profile dispersion the optimum value of $\alpha$ is given by:

**Table 2**

Pulse dispersion and bandwidth of graded-index multimode fibres

| | | | $\sigma$(ps·km$^{-1}$) | | | $B \times L$ (GHz·km) | |
|---|---|---|---|---|---|---|---|
| Process | Date | $\Delta$/% | Measured | Theory | $\sigma_{meas}/\sigma_{th}$ | Measured | Theory |
| VAD | 9/80 | 1 | 28 | 14 | 2 | 6·7 | 13·4 |
| MCVD | 3/80 | 1 | 50 | 14 | 3·6 | 3·7 | 13·4 |
| PCVD† | 1977 | 0·94 | 70 | 12·4 | 5·6 | 2·7 | 15 |
| OVPO | 1/78 | 0·76 | 60 | 8·1 | 7·5 | 3·1 | 23 |

† An inside vapour-phase oxidation process in which a microwave plasma is generated in the reacting gases.

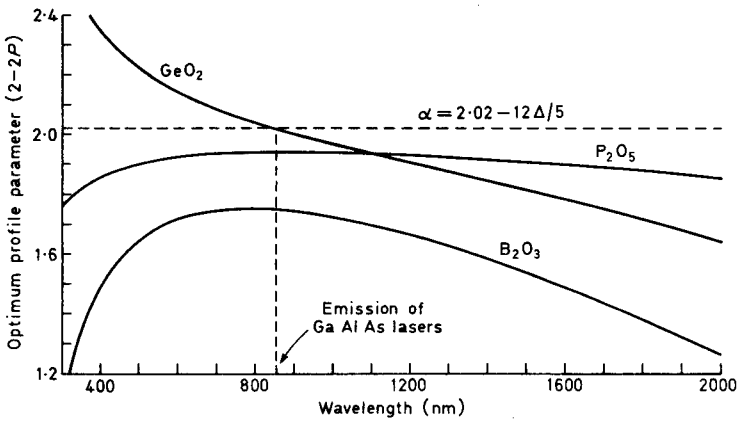


**Fig. 7.** Variation of the optimum profile parameter for germanosilicate, phosphosilicate and borosilicate glasses. The broken horizontal line represents the profile grading function $\alpha = 2{\cdot}02 - 12\Delta/5$ which, for germanosilicate glasses, is optimum for operation at 850 nm.

$$\alpha_{opt} = 2 - 2P - 12\Delta/5 \tag{19}$$

where the profile dispersion parameter $P$ is defined as

$$P(\lambda) = \frac{n_1}{N_1}\frac{\lambda}{\Delta}\frac{d\Delta}{d\lambda} \tag{20}$$

Equation (19) is only valid if the grading function is constant, i.e. if $\alpha$ is independent of wavelength. $P$ is then purely a property of the additive (e.g. germania) employed to modify the index of the base glass (e.g. silica) and does not depend on the dopant concentration. Unless this is the case, $P$ varies across the core of a graded-index fibre and an $\alpha$ profile is not the optimum for equalizing the mode transit times.[27] $P$ would thus be a meaningless parameter.

The most reliable measurements[28] of $P$ for the germanosilicate system show no dependence on concentration. The results are shown in Fig. 7 in the form of curves of $(2-2P) = (\alpha_{opt} + 12\Delta/5)$ versus wavelength. The figure also includes similar results for the other two most important dopants in silicate fibres, namely phosphorus pentoxide and boric oxide.

It may be seen from Fig. 7 that $\alpha_{opt}$ is a strong function of wavelength, particularly for germania and boric oxide dopants. It follows that a profile optimized for one wavelength is, in general, inappropriate for operation at another source wavelength. Intermodal dispersion is therefore a function of wavelength. For example, a germania-doped fibre having a profile parameter of $(2{\cdot}02 - 12\Delta/5)$.(represented as a horizontal line in Fig. 7) would have least intermodal dispersion at the wavelength, 0·85 μm, where the curve of $2-2P$ falls to $(2{\cdot}02 - 12\Delta/5)$. With departure from $\lambda = 0{\cdot}85$ μm the profile is no longer optimal and the bandwidth thus decreases rapidly. Close control of the fabrication process is therefore required in order to ensure that the highest bandwidth occurs at the intended operating wavelength.

It is desirable to produce fibres having large bandwidths over a broad spectral range. This would extend the capacity of the fibre by allowing operation at several wavelengths simultaneously (wavelength-division multiplexing) and give the user the flexibility of altering the source wavelength if improved devices become available after the installation of a cable. Fibre designs employing more than one index-modifying additive have been proposed which either reduce the wavelength-dependence of bandwidth over a particular spectral range, or optimize the intermodal dispersion for several different operating wavelengths.

### 4.4 Material Dispersion in Multimode Fibres

The power carried by multimode fibres travels almost entirely in the core region. Because, in addition, most modes are operated far from cut-off they are almost free of waveguide dispersion. The pulse delay in multimode fibres is thus given, to first order, by[8]

$$\tau = \frac{L}{c}N_1 = \frac{L}{c}\left(n_1 - \lambda\frac{dn_1}{d\lambda}\right) \tag{21}$$

where $N_1$ is the group index of the core material. (For graded-index fibres, $N_1$ represents a value of group index averaged over the core area.)

Semiconductor sources used in optical communications systems radiate over a finite range of wavelengths and, from equation (21), each spectral component travels at a different group velocity. The resulting pulse broadening $\sigma_m$ is known as material dispersion.

For a source of r.m.s. spectral width $\sigma_s$ and mean wavelength $\lambda_s$, $\sigma_m$ may be evaluated by expanding equation (21) in a Taylor series about $\lambda_s$:

$$\sigma_m = \sigma_s\frac{d\tau}{d\lambda} + \frac{\sigma_s^2}{2!}\frac{d^2\tau}{d\lambda^2} + \ldots \tag{22}$$

The first term normally dominates, particularly for sources operating in the 0·8 to 0·9 μm wavelength region. Thus for the material illustrated in Fig. 4(b) the material dispersion parameter $M = \frac{1}{L}\frac{d\tau}{d\lambda}$ is $\sim 100\text{ps nm}^{-1}\text{ km}^{-1}$ at 0·85 μm. For a typical light-emitting diode having

$\sigma_s = 18$ nm and $\lambda_s = 850$ nm the resulting pulse broadening is 1·8 ns·km$^{-1}$ which limits the $B \times L$ product to 100 MHz·km. This level of dispersion is an order of magnitude greater than the intermodal dispersion in the best available fibres. Even with semiconductor lasers (having spectral widths of, typically, 1 nm r.m.s.), material dispersion sets an ultimate limit on the capacity of optical fibre systems.

Figure 4(b) shows that a wavelength region exists where the material dispersion parameter is negligible. The wavelength $\lambda_m$ of zero material dispersion is found to vary according to the glass composition[29] but, for silica-based fibres, is always in the vicinity of 1·3 μm. Operation in this wavelength region substantially reduces the bandwidth limitations arising from material dispersion and very high $B \times L$ products are available, even with light-emitting diodes. It may be seen from Fig. 3 that, for silica-based glasses, the fibre attenuation is also extremely low (0·38 dB·km$^{-1}$).

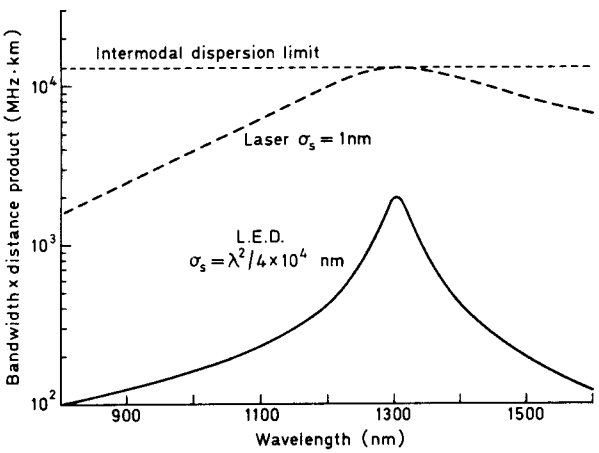


**Fig. 8.** Bandwidth limitation resulting from material dispersion in a typical $GeO_2-P_2O_5-SiO_2$ multimode fibre (see Fig. 4(b) for dispersion data). The dashed curve applies to a semiconductor laser source having a spectral width of 1 nm r.m.s. The solid line is for a typical l.e.d. having a spectral width given by $\lambda^2/4\times10^4$ nm. For a numerical aperture of 0·2 ($\Delta \simeq 1\%$), residual intermodal dispersion alone limits the $B \times L$ product to the value shown by the dotted line.

As shown in Fig. 8, the bandwidth available from multimode fibres increases rapidly as the wavelength of operation is increased from 0·85 μm (emission of GaAlAs devices) to the region of negligible material dispersion ($\sim$ 1·3 μm). Thus for a laser having a spectral width of 1 nm r.m.s. (dashed curve), the information-carrying capacity is limited in the region of 1·3 μm, by residual intermodal dispersion. For a numerical aperture of 0·2 the maximum available bandwidth is $\sim$ 13 GHz·km, providing the refractive-index profile is correctly designed. A large proportion of future multimode systems will therefore be operated at 1·3 μm.

Material dispersion does not completely vanish, however, even at the wavelength where the first derivative of group delay $d\tau/d\lambda$ is zero. According to equation (22) higher-order terms must then be taken into account.[30] The pulse broadening resulting from second-order material dispersion is proportional to the square of the source linewidth, and for silica-based fibres is of the order of 0·1 ps·nm$^{-2}$ km$^{-1}$. With laser sources second-order material dispersion is not a serious limitation.

The linewidth of light-emitting diodes increases as the square of the operation wavelength[31] and, at 1·3 μm, values of 100 nm f.w.h.m. (42 nm r.m.s. spectral width) have been reported. With such broad spectral widths, second-order material dispersion limits the bandwidth[32] to about 2 GHz·km$^{-1}$, see Fig. 8, solid curve. Although the bandwidth of the best multimode fibres can, in principle, be limited in this way, in practice a counteractive effect, namely wavelength filtering,[31,33] takes place. The latter effect results from even minor variations in the loss/wavelength characteristic of the fibre, which are enhanced by transmission over long distances (e.g. 20–30 km for typical 1·3 μm systems). Thus, the effective wavelength spread is dictated[31,33] more by the attenuation characteristics of the fibre than by the spectral width of the source. In addition the wavelength at which the received power is a maximum may not coincide with the peak source wavelength.

### 4.5 Sources for Multimode Fibre Systems

Semiconductor sources developed for optical communications are of two types, namely injection lasers and light-emitting diodes. Semiconductor lasers allow 1 mW or more to be launched into multimode fibres. With surface-emitting l.e.d.s launched power levels of a few hundred microwatts have been achieved. With edge-emitting, high-radiance, l.e.d.s, up to 1 mW of power can be launched into typical multimode fibres. Unfortunately l.e.d.s having large output power usually have a reduced modulation bandwidth. Semiconductor lasers offer better performance than l.e.d.s; their cost is, however, much greater than for l.e.d.s and their reliability is still not sufficient for some systems applications. Both types of device are therefore used in the systems already installed, or planned, for the near future.

## 5 Conclusions

In the short space of 15 years optical fibre transmission lines have been transformed from a tentative research idea to practical realization. Optical fibre cables are already in operation in the trunk telephone network and a massive extension of their use is planned which includes submarine cable communication. The attenuation attainable is nearly two orders of magnitude lower than in coaxial cable and the bandwidth of single-mode fibres is four orders of magnitude greater.

A variety of fibre types are available commercially, ranging from single-mode fibres having a core diameter of a few micrometres to step-index, plastic-cladded,

multimode fibres approaching 1 mm diameter. Applications to short-distance links such as in buildings, aircraft and between computers are being studied, as well as in instrumentation for current measurement at high voltages, in fibre gyroscopes and in hazardous situations such as fuel tanks and other explosive atmospheres where metal conductors cannot be used. The extension of 'electronic' techniques to optical wavelengths is well under way.

## 6 References


1 Midwinter, J. E., 'Optical Fibres for Transmission' (Wiley, New York, 1979).
2 Payne, D. N. and Gambling, W. A., 'New silica-based low-loss optical fibres', *Electronics Letters*, **10**, p. 289, 1974.
3 French, W. G., MacChesney, J. B., O'Connor, P. B. and Tasker, G. W., 'Optical waveguides with very low losses', *Bell Syst. Tech. J.*, **53**, pp. 951–4, 1974.
4 Sandbank, C. P. (Ed.) 'Optical Fibre Communication Systems' (Wiley, Chichester, 1980).
5 Sudo, S., Kawachi, M., Edahiro, T., Izawa, T., Shioda, T. and Gotuh, H., 'Low-OH-content optical fibre fabricated by vapour-phase axial-deposition method', *Electronics Letters*, **14**, pp. 534–5, 1978.
6 Miya, T., Terunuma, Y., Hosaka, T. and Miyashita, T., 'Ultimate low-loss single-mode fibre at 1·55 μm', *Electronics Letters*, **15**, pp. 106–8, 1979.
7 Snyder, A. W., 'Asymptotic expressions for eigenfunctions and eigenvalues of a dielectric optical waveguide', *IEEE Trans. on Microwave Theory & Techniques*, **MTT-17**, pp. 1130–8, 1969.
8 Gloge, D. 'Weakly guiding fibres', *Applied Optics*, **10**, pp. 2252–8, 1971.
9 Payne, D. N. and Gambling, W. A., 'Zero material dispersion in optical fibres', *Electronics Letters*, **11**, pp. 176–8, 1975.
10 Gambling, W. A., Matsumura, H. and Ragdale, C. M., 'Mode dispersion, material dispersion and profile dispersion in graded-index single-mode fibres', *IEE J. Microwaves, Optics & Acoustics*, **3**, pp. 239–46, 1979.
11 Adams, M. J., Payne, D. N. and Ragdale, C. M., 'Birefringence in optical fibres with elliptical cross section', *Electronics Letters*, **15**, pp. 298–9, 1979.
12 Love, J. D., Sammut, R. A. and Snyder, A. W., 'Birefringence in elliptically deformed optical fibres', *Electronics Letters*, **15**, pp. 615–6, 1979.
13 Norman, S. R., Payne, D. N., Adams, M. J. and Smith, A. M., 'Fabrication of single-mode fibres exhibiting extremely low polarization birefringence', *Electronics Letters*, **15**, pp. 309–11, 1979.
14 Gambling, W. A. and Matsumura, H., 'Simple characterisation factor for practical single-mode fibres', *Electronics Letters*, **13**, pp. 691–3, 1977.
15 Snyder, A. W., 'Excitation and scattering of modes on a dielectric or optical fiber', *IEEE Trans. on Microwave Theory & Techniques*, **MTT-17**, pp. 1138–44, 1969.
16 Gambling, W. A., Matsumura, H. and Ragdale, C. M., 'Joint loss in single-mode fibres', *Electronics Letters*, **14**, pp. 491–3, 1978.
17 Petermann, K. 'Fundamental mode microbending loss in graded-index and W fibres', *Optical & Quantum Electronics*, **9**, pp. 167–79, 1977.
18 Miyagi, M. and Yip, G. L., 'Mode conversion and radiation losses in a step-index optical fibre due to bending', *Optical & Quantum Electronics*, **9**, pp. 51–60, 1977.
19 Gambling, W. A., Matsumura, H., Ragdale, C. M. and Sammut, R. A., 'Measurement of radiation loss in curved single-mode fibres', *IEE J. Microwaves, Optics & Acoustics*, **2**, pp. 134–40, 1978.
20 Gambling, W. A., Matsumura, H. and Ragdale, C. M., 'Curvature and microbending losses in single-mode optical fibres', *Optical & Quantum Electronics*, **11**, pp. 43–59, 1979.
21 Sasaki, I., Payne, D. N., Mansfield, R. J. and Adams, M. J., 'Variation of refractive index profiles in single-mode fibre preforms measured using an improved high-resolution spatial-filtering technique', 6th European Conference on Optical Communication, York 1980.
22 Snyder, A. W. and Sammut, R. A., 'Fundamental ($HE_{11}$) modes of graded optical fibres', *J. Opt. Soc. Am.*, **69**, pp. 1663–71, December 1979.
23 Stewart, W. J., 'Simplified parameter based analysis of single-mode optical fibres', *Electronics Letters*, **16**, pp. 380–2, 1980.
24 Matsumura, H., Suganuma, T. and Katsuyama, T., 'Simple normalization of single-mode fibres with arbitrary index profile', 6th European Conference on Optical Communication, York 1980.
25 Gloge, D. and Marcatili, E. A. J., 'Multimode theory of graded-core fibres', *Bell Syst. Tech. J.*, **52**, pp. 1563–78, 1973.
26 Olshansky, R. and Keck, D. B., 'Pulse broadening in graded-index optical fibres', *Applied Optics*, **15**, pp. 483–91, 1976.
27 Arnold, J. A., 'Optimum profiles for dispersive multimode fibres' *Optical & Quantum Electronics*, **9**, pp. 111–9, 1977.
28 Sladen, F. M. E., Payne, D. N. and Adams, M. J., 'Profile dispersion measurements for optical fibres over the wavelength range 350 nm to 1900 nm'. Proceedings of 4th European Conference on Optical Communication, pp. 48–57, Genoa 1978.
29 Payne, D. N. and Hartog, A. H., 'Determination of the wavelength of zero material dispersion in optical fibres by pulse-delay measurements', *Electronics Letters*, **13**, pp. 627–9, 1977.
30 Kapron, F. P., 'Maximum information capacity of fibre-optic waveguides', *Electronics Letters*, **13**, pp. 96–7, 1977.
31 Gloge, D., Ogawa, K. and Cohen, L. G., 'Baseband characteristics of long-wavelength led systems', *Electronics Letters*, **16**, pp. 366–7, 1980.
32 Adams, M. J., Payne, D. N., Sladen, F. M. E. and Hartog, A. H., 'Optimum operating wavelength for chromatic equalisation in multimode optical fibres', *Electronics Letters*, **14**, pp. 64–6, 1978.
33 Stewart, W. J., 'Wavelength filtering effects in multimode fibres', Proceedings of Optical Communication Conference, Paper 12.3, Amsterdam 1979.


*Manuscript received by the Institution on 20th February 1981.*
*(Paper No. 1994/Comm 221)*

# Some Recent Optical Fibre Developments—1

## Cable Television and Radio over Optical Fibres

To demonstrate the suitability and advantages of fibre optics over conventional wire systems for carrying cable colour television and stereo radio signals, twenty optical fibre systems have been supplied by Standard Telecommunication Laboratories (STL) to British Telecom's Martlesham Heath laboratories.

These broadband optical fibre transmission systems comprise two sections: the trunk transmission system between the receiving aerial and a distribution switch, and a number of links from the distribution switch to subscribers. The trunk equipment consists of five similar single fibre systems. Using pulse frequency modulation four of these each carry one colour television channel, including television sound, while the fifth carries three v.h.f. stereo radio channels.

For the purposes of the demonstration the number of subscribers served has been limited to seven. Each subscriber link consists of two fibres and can simultaneously carry two television channels or six radio channels. A pair of ordinary metallic wires allows each subscriber to select the desired programme by controlling the distribution switch.

This type of transmission equipment is very similar to that which can be used in an interactive broadband network. British Telecom is planning such a system for a trial two-way visual service which will link 50 subscribers in three UK cities in 1982.

Optical fibre for the Martlesham demonstration system was supplied by STL's parent company, Standard Telephones and Cables. British Telecom provided the video distribution switch. Transmit/receive modules are now being manufactured by ITT Components — part of STC — in Leeds. Systems will be marketed by STC transmission products division from Basildon, Essex.

## Connectors for Fibre Optics

Plessey Connectors of Northampton have recently launched a lens type fibre optic connector and a prototype fibre optic DIN 41612 insert. The advantages of the lens type connector are most apparent when very reliable connectors are required to work in extreme environmental conditions. In the lens type connector all the precision parts are contained behind the hard sapphire sphere lens within the connector body and are not exposed to the environment. The lens type connector is robust, easy to clean, repeatable and reliable, and for systems requiring frequent use in adverse conditions is more cost effective.

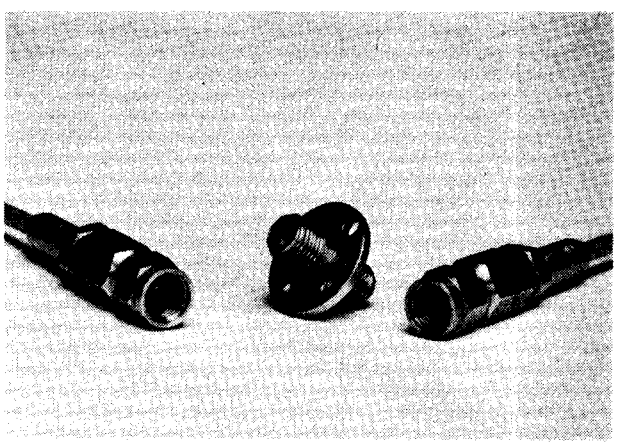

The lens type fibre optic connector developed by Plessey Connectors

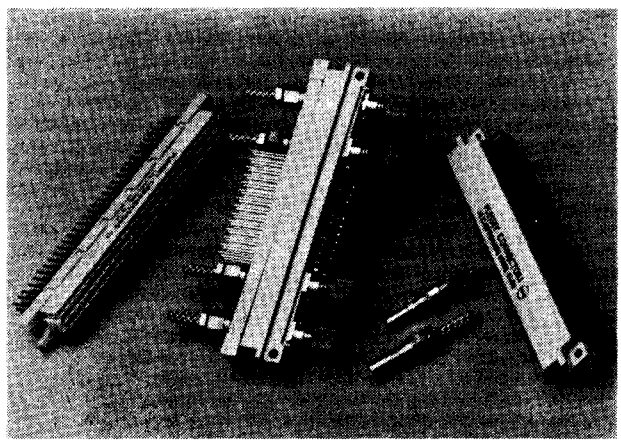

Centre: A mated new version of the Series 16 with fibre optic DIN 41612 insert
Left and right: Plessey Connectors new version of the Series 16

Based on the experience of the Plessey ferrule connector type FC701, ferrule inserts are being developed to fit existing connector bodies. These inserts will enable low loss connection of optical fibres in multiway or mixed optical/copper combinations. This type of connector insert is being used with the Series 16 range of connectors which was introduced to meet the market requirement for reliable cost effective indirect interconnections between printed circuit boards or between associated printed circuit boards and backplanes.

## Optical Fibre Fault Locator and Attenuation Measuring Set

Cossor Electronics has recently introduced a new optical fibre fault locator. Using time domain reflectometry techniques, the instrument can be used for the detection of faults, joints and other imperfections in optical fibres and cables. It complements Cossor's range of conventional cable fault locators and, like them, it is compact (measuring $140 \times 260 \times 290$ mm), lightweight (7·5 kg) and fully self-contained, with an internal battery pack which gives in excess of eight hours continuous use.

The instrument has a screen displaying a complete view of the cable under test, which gives an indication of the type of fault. Areas of particular interest on the display can be expanded for greater detail. Attenuation assessment is facilitated by etched reference lines on the screen. In addition, a direct digital readout, in metres, of distance to a fault is provided for accurate measurement. The maximum measurement range is 10 km and fibre core diameters from 50 μm upwards can be accommodated.

In conjunction with the optical fibre fault locater, Cossor has also introduced an optical fibre attenuation set. It is a two-part, field-portable, battery powered, instrument, comprising a transmitter and receiver for measuring optical path losses up to 60 dB. The transmitter and receiver can be carried in detachable halves of a briefcase-style container, which also houses the accessories.